

1 Cotton Fabrics Coated with Few-Layer Graphene as Highly 2 Responsive Surface Heaters and Integrated Lightweight Electronic- 3 Textile Circuits

4 Housseinou Ba,* Lai Truong-Phuoc, Vasiliki Papaefthimiou, Christophe Sutter, Sergey Pronkin,
5 Armel Bahouka, Yannick Lafue, Lam Nguyen-Dinh, Giuliano Giambastiani,* and Cuong Pham-Huu*



Cite This: <https://dx.doi.org/10.1021/acsnm.0c01861>



Read Online

ACCESS |



Metrics & More



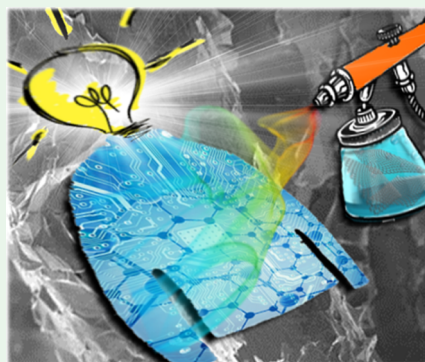
Article Recommendations



Supporting Information

6 **ABSTRACT:** In this work, we describe an eco-friendly and cost-efficient method for
7 the production of highly dispersed few-layer graphene solutions using karaya gum as a
8 bioinspired exfoliating agent. The as-synthesized graphene aqueous solutions can be
9 easily applied on a cotton cloth through dip- or brush-coating, thanks to the interaction
10 between the graphene sheets decorated with the gum and the functional groups on the
11 cotton cloth host substrate surface. The as-prepared fabric composites display high
12 mechanical stability, anchorage, and high electrical conductivity that make them
13 excellent candidates within a relatively high number of technological applications. The
14 study mainly focuses on the potentialities of cotton fabric composites as planar heating
15 devices or electronic-textile (e-textile) circuits prepared by postlaser treatment. By
16 means of a laser beam, local graphitization or partial etching of the graphene conductive
17 lines can be achieved to generate conductive areas with different resistances, which can
18 act as flexible and integrated electronic circuits. Besides lightweight conductive circuits,
19 the graphene-coated cotton fabrics were experimentally tested for other technological
20 applications, that is, as flexible metal-free markers or for IR shielding or as nonflammable barriers for the protection of sensitive
21 devices or to prevent flame spreading. This technology allows one to open a new route toward the development of daily life
22 connected and flexible e-textile devices of added value with low carbon footprint impact.

23 **KEYWORDS:** *few-layer graphene, cotton cloth, e-textiles, laser patterning, composite*



1. INTRODUCTION

24 Electronic textiles (e-textiles) represent a novel type of high-
25 tech products resulting from the integration of complex
26 electronic structures and common textiles. They can find
27 applications in several areas ranging from the production of
28 biomedical,^{1–3} sensing⁴ and power generation, or energy
29 storage devices^{5–8} to addressable wiring devices for everyday
30 needs.⁹ Different technologies have been developed until now
31 for the production of e-textiles, and they can include
32 embroidering, knitting, weaving, spinning, braiding, coating,
33 printing, and chemical treatment.¹⁰ Depending on their
34 downstream applications (i.e., wearable displays, portable
35 power systems, high-performance sportswear, or health-
36 monitoring devices),^{11–13} e-textiles should maintain key
37 properties such as high flexibility and stretchability, light-
38 weight, and high resistance toward leaching upon their
39 washing. The fabrication of e-textiles relies on the homoge-
40 neous coating of a textile support by an efficient layer of a
41 conductive material which confers electrical conductivity to the
42 composite. Cotton cloth is a flexible and hierarchical porous
43 support made of natural cotton fibers, which displays a
44 relatively high thermal resistance and can be used as a

macroscopic host matrix for the deposition of a conductive
45 layer. Other advantages of the cotton fabric are due to its
46 economic processability and mechanical and flexible proper-
47 ties.^{14–16} The cotton cloth also displays numerous functional
48 groups such as hydroxyl and carbonyl functionalities on its
49 surface, which provide anchorage sites for linking with the
50 deposited conductive graphene layer, hence improving the final
51 mechanical strength of the coated composite.¹⁷ According to a
52 recent review article on e-textiles and their application areas,¹⁸
53 there is still a lot of room available for improving this
54 technology, especially regarding the large scale-up production
55 of these composites. Recently, Novosolov and co-workers
56 described an interesting technique for the scalable production
57 of e-textiles based on the pad-dry deposit of a thin layer of
58 reduced graphene oxide (rGO) on the surface of a host
59

Received: July 9, 2020

Accepted: August 31, 2020

Published: August 31, 2020

60 matrix.¹⁹ The potential manufacturing rate of e-textiles by this
61 technique was estimated to be ≈ 150 m/min using the already
62 existing industrial production method. In addition, their
63 electrical conductivity was made variable as a function of the
64 number of depositing cycles, hence varying the number of rGO
65 layers deposited on the textile fibers. However, the use of rGO
66 can face with some technical limitations, especially because of
67 the tedious and less than trivial synthesis of both GO and rGO
68 materials. The use of hydrocolloids for the production of
69 exfoliated graphene and few-layer graphene (FLG) sheets has
70 received growing interest compared to that of organic solvents,
71 especially because of their reduced environmental impact.^{20,21}

72 Graphene and FLG are two-dimensional (2D) conductors
73 with a high effective surface area as well as chemical stability
74 along with high mechanical strength and flexibility. These
75 unique properties have made it possible to employ them in a
76 number of high-technological applications during the past
77 decades.^{22–28} Graphene and related materials were also
78 extensively investigated as transparent heaters^{29–32} in place
79 of metal nanowires. However, for graphene suspended in liquid
80 media, classically produced through the liquid-phase exfolia-
81 tion (LPE) process, aggregation or restacking phenomena
82 rapidly occur because of high van der Waals attraction forces
83 between single or few graphene layers, which render its
84 processability rather hard if not impossible.^{33–35} Such a
85 problem is not encountered with graphene produced through
86 chemical vapor deposition, followed by transfer to the host
87 substrate. Anyway, the high surface energy of the graphene
88 sheets confers them a high tendency to wrap foreign structures
89 upon contact, followed by a drying step. This property is of
90 high interest for the preparation of graphene/macroscale
91 composites with potential applications in the field of detection
92 or electrically conductive devices.

93 This property has prompted us to combine FLG sheets with
94 a macroscale host support such as a cotton fabric to provide
95 composite materials with potential applications in several
96 technological areas such as electronics, health care, wearable
97 cloths, sensors, and heating and power storage devices.^{13,36–38}
98 As far as industrial applications of these composites are
99 concerned, they should be produced on a large scale under
100 green conditions and with the lowest costs in order to reduce
101 the problems linked with the postsynthesis purification paths.
102 In addition, the conductive coating layer should not imply
103 health and security issues during its fabrication as well as
104 during the composite processing. This is the case of cotton
105 fabrics functionalized with carbon nanotubes (CNTs). For the
106 latter, health and safety issues linked to their ultimate use^{39–41}
107 remain a matter of debate within the scientific community.

108 In this work, we describe the straightforward production of
109 e-textiles from a commercial cotton matrix by its coating with
110 an aqueous suspension of FLG sheets. The FLG synthesis was
111 carried out in a water medium, that is, 98%, containing a
112 biocompatible exfoliant and under room temperature (rt),
113 which significantly reduces the environmental impact and the
114 overall cost of the process. In general, LPE of raw graphite to
115 produce graphene or FLG sheets is generally based on the use
116 of various organic solvents such as *N,N*-dimethylformamide,
117 *ortho*-dichlorobenzene, 1-methyl-2-pyrrolidone, benzyl ben-
118 zoate, acetophenone, benzonitrile, dimethyl sulfoxide, or
119 dioxane.⁴² All these solvents are toxic and expensive and
120 generally possess high boiling points, and thus, their large-scale
121 use raises important environmental concerns. All these solvents
122 need special handling precautions during the exfoliation

procedure, and liquid or gaseous phases resulting from the
123 processing method need to be treated as they cannot be
124 released as such in the environment. Accordingly, LPE in a
125 water medium significantly reduces the environmental impact
126 of the process, while the lack of postsynthesis treatment of
127 volatile organic compounds contributes to the reduction of the
128 process costs. During the deposition and drying steps, only
129 steam was released. This feature simplifies significantly the
130 postprocess gaseous treatment compared to that encountered
131 with organic solvents. As a result, LPE in the water medium,
132 with or without additives, represents an interesting alternative
133 to the production of graphene-based materials for different
134 downstream applications.^{43,44} The as-prepared composites
135 have been successfully applied as low-energy-consuming and
136 fast heat on/off switchable heaters as well as flexible textile-
137 based composites to produce electronic circuits through laser
138 patterning paths. They displayed a highly flexible behavior
139 together with an extremely high electrical conductivity and
140 durability against repeated bending or scrolling treatments.
141 This latter feature is expected to reduce significantly all main
142 issues related to material loss/alteration upon use, hence
143 limiting any accidental breathing of hazardous particles from
144 potential end users. The effect of FLG sheet concentration in
145 the aqueous medium has also been investigated with respect to
146 the electrical conductivity of produced e-textiles, and the
147 results obtained on optimized samples have been thoroughly
148 discussed. Laser patterning of e-textiles has also been applied
149 either to generate integrated electronic circuits with a high
150 lateral resolution or to prepare electronic tracks featured by
151 variable electrical resistance for replacing metal compounds
152 and plastics usually used nowadays which pose problems for
153 the environment both in terms of production and in terms of
154 waste disposal. The laser patterning of e-textiles for the
155 production of electronic circuits of variable dimensions and
156 featured by e-tracks with different resistances has only few
157 precedents in the literature, especially for the manufacture of
158 flexible and lightweight metal-free electronic circuits. Indeed, e-
159 textiles are generally produced in the form of a single and
160 homogeneous composite showing a similar resistance through-
161 out the whole sample. Finally, FLG-coated cotton cloths have
162 been successfully used as efficient flame retardants or flame
163 barriers suitable for preventing fire spreading. 164

2. MATERIALS AND METHODS

2.1. FLG Synthesis. Karaya gum obtained from *Sterculia urens* was
165 employed as a green exfoliating agent to synthesize FLG sheets from
166 expanded graphite (EG) in aqueous solution. Karaya gum is a highly
167 water-soluble polysaccharide also known as a highly charged (ionic)
168 hydrocolloid, and it consists of galactopyranose ($\sim 44\%$), arabinopyr-
169 anose/arabinofuranose ($\sim 25\%$), rhamnopyranose ($\sim 14\%$), glucur-
170 opyranosyl uronic acid ($\sim 15.5\%$) together with 4-*O*-methyl
171 glucuropyranosyl uronic acid ($\sim 1.5\%$), and a small amount ($\sim 2\%$)
172 of proteins, which can be summarized into aromatic rings linked to
173 oxygen functional groups.^{45,46} Its exfoliation power is basically
174 ascribed to the ability of the hydrophobic polypeptide chains of the
175 gum to be adsorbed at the graphene surface through van der Waals
176 interactions (π - π stacking interactions mainly), while branched
177 hydrophilic O-containing moieties ensure a good dispersion of the
178 mechanically exfoliated graphene sheets in the aqueous medium.
179

For exfoliation experiments, an amount of 5 g of EG (as a starting
180 raw material) and 0.5 g of karaya gum (as both a natural emulsifying
181 agent and stabilizing agent) were added to 500 mL of distilled water.
182 The exfoliation process was carried out in a Branson digital sonifier
183 (SFX550 model made by Emerson Co., featuring with a nominal
184 power of 400 W at 20 kHz and equipped with a 1/2" disruptor horn) 185

186 operating at a power of 40 W (10% of the nominal power) at rt for 2
187 h. The mixture was continuously stirred (300 rpm) while maintaining
188 its temperature constant at rt by means of an external cooling device.
189 During the sonication process, cavitation micrometer bubbles are
190 formed in the liquid phase. The bubble collapse induced by cavitation
191 releases intense local energy, that is, a temperature of 5000 °C and a
192 local pressure exceeding several hundred atmospheres,⁴⁷ which break
193 down the loosely connected EG to yield graphene and FLG or
194 ultrathin graphite flakes. The as-formed graphite-based materials were
195 stabilized through surface interaction by the karaya gum, thus forming
196 stable suspensions in the liquid medium.

197 Different concentrations of FLG in the aqueous suspension (from 2
198 to 10 g/L) were used depending on the composite downstream
199 application. The nanostructures and morphologies of the as-
200 synthesized products were investigated by scanning electron
201 microscopy and transmission electron microscopy (SEM and
202 TEM). SEM and TEM micrographs clearly showed the presence of
203 highly dispersed micrometer-sized FLG sheets generally formed by
204 less than 20 stacked layers. The number of stacked graphene sheets
205 and the nature of the surface functional groups were also analyzed by
206 Raman spectroscopy and X-ray photoelectron (XP) spectroscopy
207 (XPS).

208 **2.2. Synthesis of FLG-Coated Cotton Cloth Composites**
209 **(FLG@CC).** The synthesis of FLG-coated cotton cloth composites
210 (FLG@CC) was accomplished through two methodologies: paint
211 brushing and dip coating. With the former method, the FLG water
212 solution was deposited on the cotton cloth using a paint brush; hence,
213 FLG sheets (5 g/L) were deposited on the painted material face only.
214 With the latter method (dip coating), the cotton cloth was soaked
215 with an aqueous solution of dispersed FLG (5 g/L), and hence, its
216 whole matrix was coated by FLG. Regardless of the method used, the
217 FLG deposit step can be repeated at will to get composites with
218 variable FLG loading. After each application, samples were heated to
219 dryness in an oven at different temperatures, 100–200 °C, for 30 min
220 to desorb all moisture and to strengthen the wrapping of the host
221 substrate by an FLG layer.

222 The cotton cloth was purchased from IKEA Inc., and its
223 composition was in line with that of traditional cotton cloths:⁴⁸
224 cellulose (94%), proteins/pectins (2%), minerals (1%), waxes/
225 organics (1.5%), and others (1%). Different types of cotton cloths
226 can be used (in principle) for the preparation of the relative
227 composites. It is formed by linear chains of thousands of $\beta(1-4)$ -
228 linked D-glucose units,⁴⁹ and the interaction with FLG sheets naturally
229 occurs (covalently) because of the adhesive properties of the
230 exfoliating agent available at the surface of FLG sheets (karaya
231 gum). The gum acts as a hydrophilic glue and ensures excellent
232 adhesion at the graphene coating.⁵⁰ Additional binding could also be
233 formed between the bonding from the oxygenated functional groups
234 present on both surfaces as well.

235 **2.3. Characterization Techniques.** SEM was carried out on a
236 ZEISS 2600F with a resolution of 5 nm. Samples were deposited onto
237 a double-face graphite tape in order to avoid charging effects
238 throughout the analysis. TEM was carried out on a JEOL 2100F
239 working at an accelerated voltage of 200kV, equipped with a probe
240 corrector for spherical aberrations and with a point-to-point
241 resolution of 0.2 nm. To prevent restacking phenomena of FLG,
242 the suspension did not undergo any intermediate drying process, but
243 it follows the following sample preparation method: 1 mL of the FLG
244 aqueous suspension was diluted with 5 mL of ethanol, and the
245 suspension was subjected to sonication for 5 min. Afterward, a drop of
246 the suspension was cast on a copper grid covered with a holey carbon
247 membrane for TEM observation and evaporated to dryness in air.
248 XPS measurements were carried out using an ultrahigh vacuum
249 spectrometer equipped with a VSW Class WA hemispherical electron
250 analyzer. A monochromatic Al K α X-ray source (1486.6 eV) was used
251 as the incident radiation. Survey and high-resolution spectra were
252 recorded in the constant pass energy mode (90 and 44 eV,
253 respectively). The CasaXPS program with a Gaussian–Lorentzian
254 mix function and Shirley background subtraction was employed to
255 deconvolute the XP spectra.

The Raman spectra were recorded using LabRAM ARAMIS 256
Horiba Raman spectrometer equipment. The spectra were recorded 257
in the range of 500–4000 cm⁻¹ using the laser excitation wavelength 258
of 532 nm. Samples were deposited on a glass substrate by dip coating 259
and carefully dried before each measurement. 260

The electrical resistance was measured by a four-point probing 261
method using a potentiostat Bio-Logic SP300 (Grenoble, France) or 262
directly using a Fluke autoranging digital multimeter. 263

The water contact angle measurements were conducted using a 264
Krüss drop shape analyzer (DSA25). 265

2.4. Laser Patterning of FLG Composites and Graphitiza- 266
tion. Electronic circuits were designed using a CO₂ laser (Epilog 267
Mini, 40 W) operating in a quasi-continuous mode at the laser 268
excitation wavelength of 10.6 μ m with a 100 μ m beam trace. The 269
cleaning and track creation parameters differ from circuit to circuit. 270
All circuits are computer-drawn (CAM) using CorelDRAW as the 271
software, and files are charged in the laser device. Lines were defined 272
as the minimum, and the space between each line was set to 0.018 273
mm oriented at 0° (parallel to the horizontal line) at 1200 dpi as the 274
resolution. During the laser patterning, the cross-jet air was set at 45° 275
with respect to the scanning direction and before the laser spot to 276
remove all graphene dusts and avoid their redeposition. The spot at 277
the focus point had a diameter of 100 μ m. The scanning speeds were 278
relatively fast (from 50 to 350 mm/s), and the power output was 279
between 1 and 10 W maximum. Power outputs higher than 10 W 280
were found to damage the textiles. 281

For the graphitization process, the same laser output power, that is, 282
1–10 W, was used at a frequency of 5 kHz. The process was used to 283
heat graphene deposits to induce local graphitization phenomena 284
while preserving the underneath textile integrity. In the graphitization 285
process, the energy efficiency (expressed as J/mm) was determined by 286
tracking the value of linear energy (E_L), which was obtained by 287
dividing the power by the scan speed. The graphitization process was 288
carried out at an E_L between 0.03 and 0.12 J/mm. 289

3. RESULTS AND DISCUSSION

3.1. Synthesis and Properties of FLG@CC. EG was used 290
as a precursor for the FLG synthesis. Figure 1A (left) displays a 291
digital photo of EG on the top of an aqueous solution 292

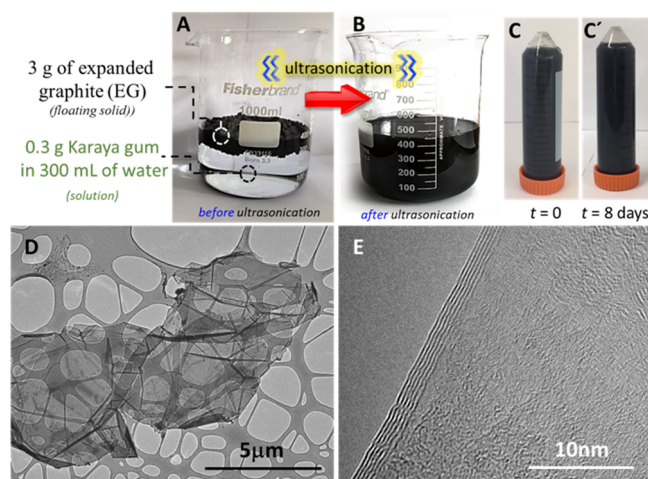


Figure 1. Process sketch for the EG exfoliation. Digital images of a batch of EG (3 g) as a floating solid in a water medium containing 0.1 wt % of karaya gum as a surfactant before (A) and after (B) the ultrasonication treatment (exfoliation process) for 2 h. (C,C') FLG solutions (10 g/L) at different settling times: $t = 0$ and $t = 8$ days, respectively. None of these homogeneous FLG dispersions show any appreciable formation of deposits. (D,E) Representative TEM micrographs of FLG after the exfoliation process at different magnifications.

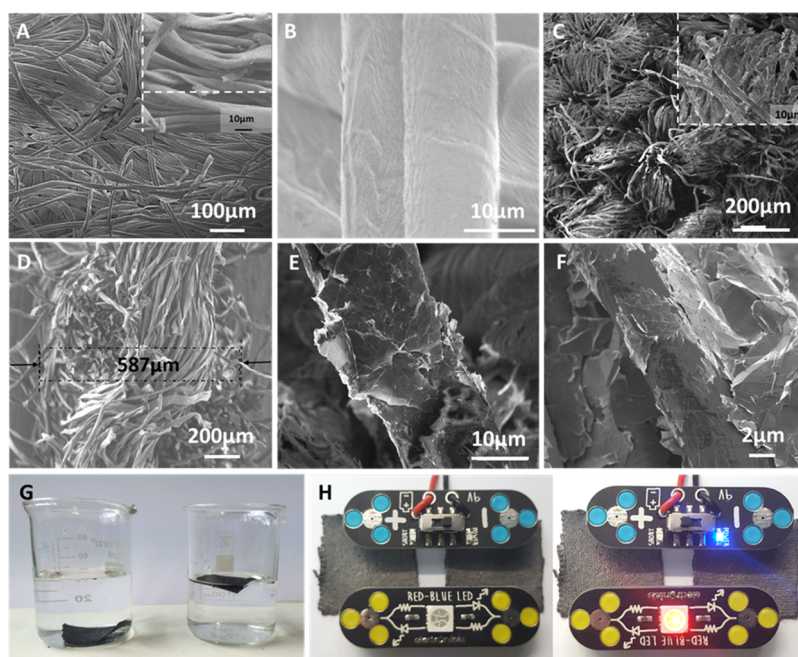


Figure 2. Representative SEM micrographs: (A,B) pristine cotton cloth showing the fibrous structure of the substrate with a smooth surface, (C,D) FLG@CC through dip and brush coating, (E,F) high-magnification view of the FLG@CC through dip and brush coating. (G) Digital photo showing the hydrophilic character of the FLG@cotton cloth treated at a low temperature (130 °C) and the same after treatment at 200 °C with a hydrophobic character. (H) Electrical conductivity of the FLG@cotton cloth assessed by a remote electrical supply device: left: off-mode, right: on-mode.

293 containing 0.1 wt % of karaya gum as an exfoliating agent (see
 294 the **Materials and Methods** section). **Figure 1A** (right)
 295 illustrates the same sample after treatment with a probe
 296 sonicator operated at 10 W and rt for 2 h. This latter picture
 297 accounts for the generation of highly and homogeneously
 298 dispersed graphite sheets in the water solution.

299 TEM micrographs of the as-obtained suspension are shown
 300 in **Figure 1B,C** and confirm the high exfoliation efficiency of
 301 the adopted protocol to give FLG sheets only, featured by less
 302 than 20 layers and a thickness < 10 nm. TEM analysis also
 303 shows the generation of relatively large graphene sheets (up to
 304 several square micrometers) that make them highly attractive
 305 materials for coating applications.

306 Indeed, the combination of large dimensions and low
 307 thicknesses allows graphene sheets to stack and even wrap
 308 around microfilaments of a given hosting matrix, hence
 309 ensuring improved mechanical stability to the final composites
 310 (*vide infra*). The high-resolution TEM micrograph (**Figure**
 311 **1C**) illustrates a representative FLG sample obtained under
 312 our exfoliation protocol that consists of six, highly crystalline
 313 graphene layers (according to the side view). Some wavy
 314 structures observed on the FLG surface are attributed to the
 315 presence of adsorbed compounds (i.e., the exfoliating agent or
 316 residues rising from the sample preparation for the TEM
 317 analysis). Looking at the relatively large distribution of FLG
 318 sheets in terms of sizes and thickness, materials should be
 319 properly named ultrathin graphite flakes in accord with the
 320 classification proposed by Boggild⁵¹ and based on the work of
 321 Castro Neto *et al.*⁵² carried out on graphene samples produced
 322 from 60 different producers. However, it is important to stress
 323 that the quality of graphene used depends on its ultimate
 324 application as each application needs graphene samples with
 325 different physical characteristics. The high stability of
 326 exfoliated FLG sheets is finally confirmed by only negligible

material residues settling down from the aqueous suspensions 327
 upon standing the samples per several days (**Figure 1D**). 328

As shown in **Figure 2**, SEM analysis of the cotton fabric at 329
 different magnifications has revealed a woven structure made 330
 of entangled microfilaments of a smooth surface. SEM 331
 micrographs of the cotton textile after brush or dip coating 332
 with an FLG solution are presented in **Figure 2C,D**. These 333
 latter figures reveal that cotton fibers are homogeneously 334
 coated with a thin layer of FLG and the pristine morphology of 335
 the textile is almost entirely preserved at least at low 336
 magnifications. SEM micrographs at higher magnifications of 337
 FLG@CC (**Figure 2E,F**) highlight a complete coating of the 338
 fibers by highly wrapped and shrunk FLG sheets that form a 339
 rough and interconnected graphene network all around the 340
 cellulose fibers, thus conferring an excellent electrical 341
 conductivity to the composite (*vide infra*). However, not all 342
 FLG sheets are completely wrapped around the fabric 343
 microfilaments, but some of them remain only loosely attached 344
 to those coating the microfilaments. We thought that the latter 345
 ensures a highly interconnected and conductive network all 346
 over the extension of the matrix in its downstream application,
 347 that is, metal-free and lightweight electrical textiles. The 348
 wrapping of the fabric microfilaments by a homogeneous layer 349
 of FLG sheets is not trivial because of the high entanglement of 350
 filaments in the host fabrics. 351

The SEM micrographs evidence the high wrapping of the 352
 FLG sheets around the cellulose fibers, indicating the high 353
 interaction between the two materials. The roughness of the 354
 FLG-coated cellulose fiber can also make the composite highly 355
 attractive for filtering applications. Indeed, the higher the 356
 roughness of the entangled fibers, the higher their interactions 357
 with exogenous particles, and hence, the higher the material 358
 filtration efficiency. The highly efficient coating of FLG sheets 359
 around cotton fibers can be ascribed to the generation of 360

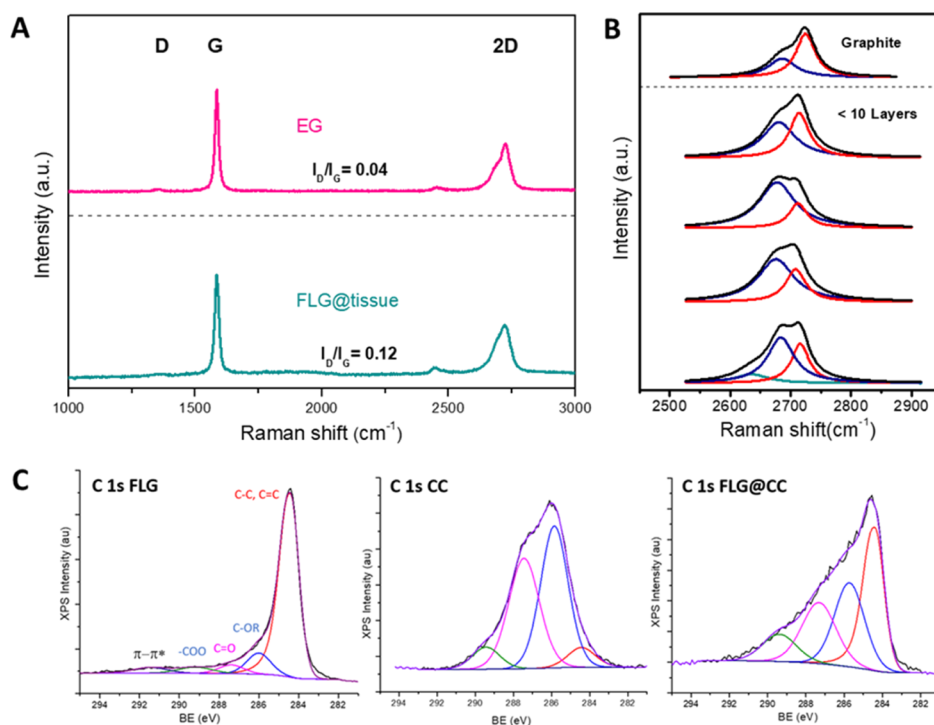


Figure 3. (A) Raman spectra of pristine EG and FLG@CC. (B) Raman spectra of exfoliated FLG showing the presence of FLG with different graphene layers. (C) Deconvoluted C 1s XPS spectra recorded on FLG, the pristine cotton cloth, and the FLG@cotton cloth showing the presence of different C–O functional groups on the sample surface.

361 strong H-bond interactions during the material drying between
 362 the functional groups of the fabric and those of the gum
 363 available on the FLG surface.^{17,53} The drying procedure allows
 364 FLG sheets to shrink around the cotton fibrils. Notably, the
 365 temperature applied during the drying step of the composite
 366 can change dramatically its surface properties. Although a
 367 drying treatment at 130 °C produces a material with a
 368 hydrophilic surface character, temperatures of 200 °C render it
 369 essentially hydrophobic in nature (Figure 2G, left vs right).
 370 Digital photos of water drops at the surface of the different
 371 FLG@CC samples (Figure S1, after coating and thermal
 372 treatment at two different temperatures) highlight the
 373 influence of the postthermal treatment on the hydrophobicity
 374 of the composites. Accordingly, a 3 wt % FLG@CC sample
 375 treated at 100 °C absorbs water as soon as drops meet its
 376 surface (Figure S1A). On the other hand, a 3 wt % FLG@CC
 377 sample treated at a temperature ≥ 200 °C highlights its
 378 improved hydrophobic character as water forms almost round-
 379 shaped drops with an average contact angle of about 130°
 380 (Figure S1B). This experiment unveiled how properties of the
 381 composites change from hydrophilic to hydrophobic upon a
 382 simple material heat treatment at relatively moderate temper-
 383 atures. According to Wang *et al.*,⁵⁴ the surface energy of the
 384 composites falls in the range of 29 ± 5 mJ·m⁻². Thus, it can be
 385 stated that the thermal treatment of FLG@CC composites
 386 reduces the wettability and decreases their interfacial adhesion
 387 with liquids. Such a result is of high interest because it
 388 demonstrates that an appropriate thermal treatment of FLG@
 389 CC samples allows to control their wettability, a feature that is
 390 crucial in the area of e-textiles. Moreover, it should also be
 391 noticed that the hydrophobicity of samples depends signifi-
 392 cantly on the textural properties of the host matrix, that is, the
 393 diameter and density of the filaments as well as the way in
 394 which they are interwoven. Unfortunately, this feature is more

challenging to be evaluated. Such a behavior can be reasonably
 attributed to the occurrence of dehydration/condensation
 processes between functionalities on cotton fibers and those of
 the gum on the exfoliated FLG sheets. Such a treatment that
 can be formally regarded as a more complete removal of
 moisture trapped between graphene sheets, increasing
 remarkably the graphene adhesion to the hosting matrix.
 This is a fundamental feature that improves the mechanical
 flexibility of the composites. According to SEM analysis,
 FLG@CC retains the mechanical flexibility of the pristine
 cotton fibers without any appreciable morphology alteration
 after repeated folding (Figure S2). Finally, a preliminary
 assessment of the electrical conductivity of FLG@CC was
 verified using a remote electrical device as shown in Figure 2H.

The Raman spectra of EG and FLG@CC are shown in
 Figure 3A and demonstrate how the graphitic degree of EG is
 almost entirely retained after the material exfoliation and
 coating of the cotton fabric. Figure 3B finally accounts for the
 2D Raman component of EG and exfoliated FLG sheets made
 of a different number of graphene layers. It should be stressed
 that coatings consist of several FLG sheets stacked one on
 another, which form a deposit with an average thickness in the
 range of few tens to hundred nanometers regardless of the
 coating process used: paint brushing or dip coating. In
 addition, such coating procedures generate films with poorer
 physical properties compared to those of a pure graphene sheet
 because of the presence of defects and irregular stacking of
 FLG sheets with randomized dimensions and thicknesses. In
 spite of this, composites prepared with the presented method
 hold physical properties that are required for their target
 application. A related work has been recently reported by
 Novoselov and co-workers for the development of a deicing
 setup obtained by coating several FLG sheets onto glass-rov-
 ing fibers through a dip-dry-cure technique.⁵⁵ Similar to our e-

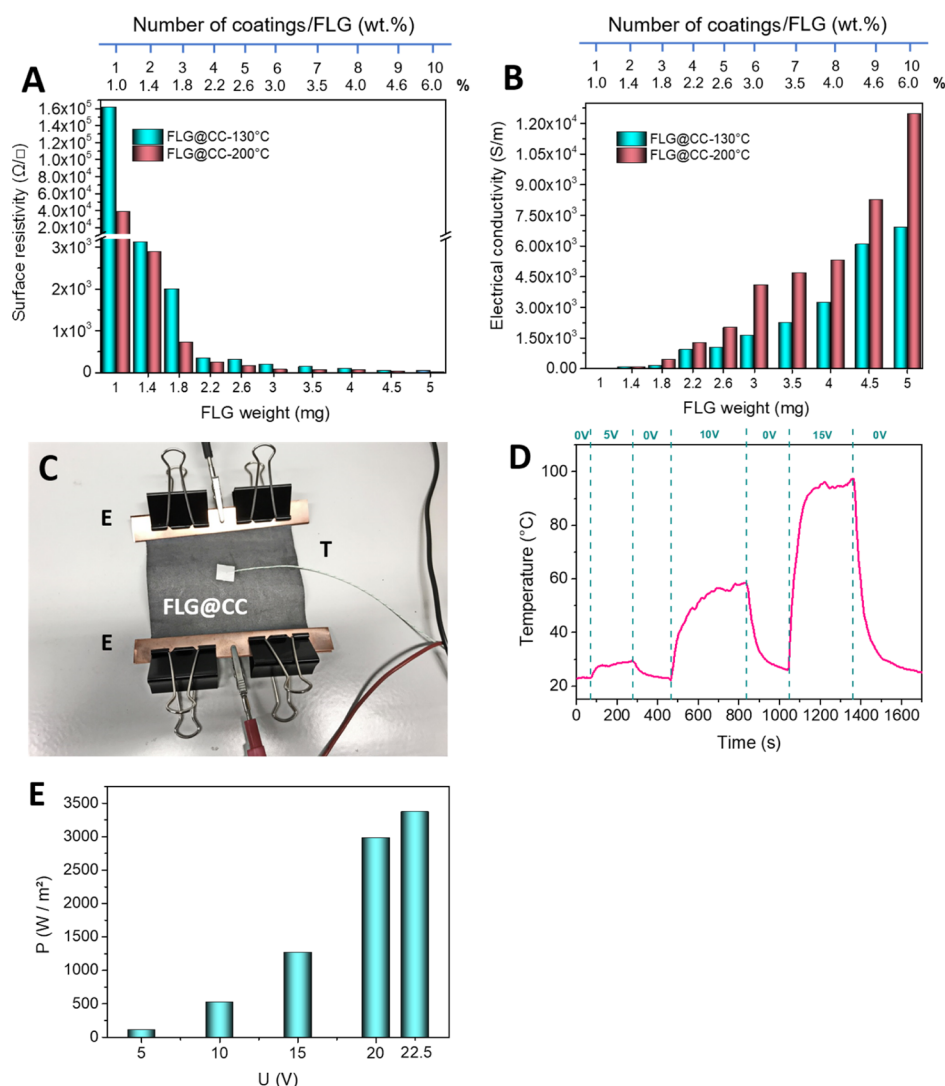


Figure 4. (A) Surface resistivity and (B) electrical conductivity as a function of coating cycles, FLG loading, and heat treatment temperature. (C) Digital photo of the device consisting a FLG@cotton cloth (13 cm \times 13 cm) for thermal property measurements: T, planar thermocouple for temperature recording; E, copper electrodes; FLG@CC, cotton cloth coated with 4 wt % of FLG after temperature treatment at 200 $^{\circ}$ C for 1 h. (D) Responsive surface temperature as a function of the applied voltage. (E) Specific power generated as a function of the applied voltage.

429 textiles, the coating presented by these authors consisted of
 430 several FLG sheets staked one on another to generate a
 431 relatively thick electrical conductive film on the glass-rovng
 432 fibers. It can be inferred that for applications such as surface
 433 heaters or electronic circuits for daily-life use, the most
 434 important issue does not rely on the production of high-quality
 435 graphene sheets but rather on the possibility to generate stable
 436 FLG sheet suspensions in the largest and simplest possible
 437 way. Catching this target opens the way to the cheap and large-
 438 scale production of metal-free, electrically conductive compo-
 439 sites. Finally, a coating technique based on the use of FLG
 440 sheets similar to that described in the present work deserves a
 441 note. In a very recent contribution, Palmieri and Papi have
 442 successfully employed FLG sheets as coating materials for the
 443 production of personal protective equipment (medical devices)
 444 or facemasks to minimize the risk of virus transmission.⁵⁶
 445 XPS results of the pristine cotton fabric are presented in
 446 Figures 3C, S3, and S4 and confirm the presence of a large
 447 amount of hydroxyl and carbonyl groups on the surface, which
 448 confers to the substrate a hydrophilic character. On the other
 449 hand, the oxygenated functional group concentration is

relatively small in the FLG sample after the exfoliation process
 according to the survey spectrum, while a large amount of such
 groups is detected on the cotton fabric surface (Figure S3).
 Oxygen decreased, while carbon increased on FLG@cotton
 cloth, which is in good agreement with the surface coating
 process. The area and position of these components are given
 in Table S1. Some small amounts of nitrogen and calcium were
 also observed on the FLG@cotton cloth XPS survey spectrum,
 which could be attributed to some impurities, issued from the
 different preparation steps, which were subsequently deposited
 onto the sample. However, such impurities are expected
 neither to play a crucial role nor to have any influence on the
 applications which will be investigated after. The non-
 deconvoluted C 1s XPS spectra of the different samples are
 presented in Figure S4 and confirm the large concentration of
 oxygenated functional groups on the pristine cotton cloth and
 almost the absence of such groups on the FLG. The C/O
 surface atomic ratios were calculated from the areas of the XPS
 peaks and were properly corrected taking into account the
 atomic sensitivity factors of each element: $C/O_{\text{FLG}} = 37.3$, $C/$
 $O_{\text{CC}} = 2.2$, and $C/O_{\text{FLG@CC}} = 4$. All C 1s XPS peaks were 470

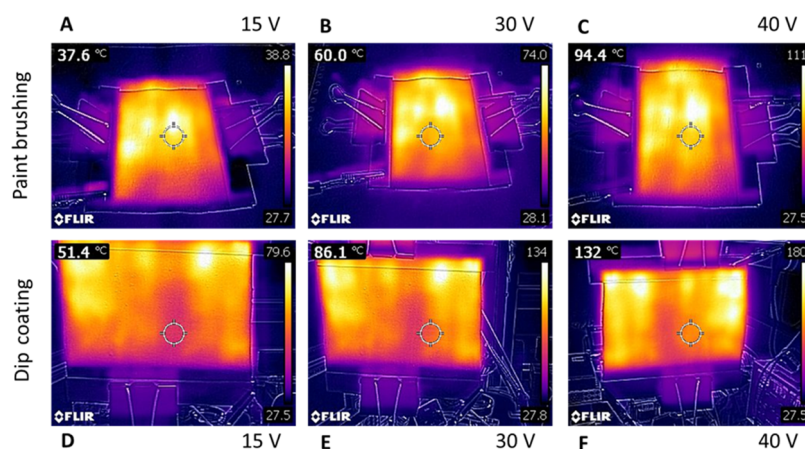


Figure 5. (A–C) Surface temperature measured using a FLIR camera of the FLG@cotton fabric (15 cm × 15 cm) composite, with an FLG loading of 2 wt %, made by paint brushing on one side of the host matrix under different applied voltages. (D–F) Surface temperature measurement using a FLIR camera of FLG@CC made through the dip-coating (both sides) process, which significantly increases the FLG deposit, with an FLG loading of 4.5 wt %, as well as the electrical conductivity, leading to a significant improvement of the surface temperature under the same applied voltage.

analyzed in four components at ca. 284.4 eV ($\text{sp}^2 \text{C}/\text{sp}^3 \text{C}$) and higher-binding-energy (BE) components that correspond to C–OR or C–N, C=O, and O–C=O and a π – π^* transition loss peak at ca. 291 eV (Figure 3C).^{57,58} The area and position of these components are given in Table S1. The O 1s peaks were analyzed in two components, that is, a high-BE component corresponding to singly bonded oxygen in carbonyls and esters and a low-BE component attributed to singly bonded oxygen in alcohols, ethers, and epoxies (Figure SS).

The anchorage stability of the FLG@CC composite was also evaluated by immersing the sample in a mixture of ethanol/water (20:80 v/v %), followed by a sonication step for 30 min at rt. The digital photos of the samples before and after sonication are displayed in Figure S6 and confirm the complete retention of FLG in the composite as no trace of any FLG was found in the supernatant solution.

3.2. Electrical Conductivity Measurements of FLG@CC e-Textiles. The surface resistivity (in Ω/\square) and electrical conductivity (S/m) of the FLG@CC e-textile after heat treatment at 130 °C for 15 min for each deposition were measured using a four-point probe, and the results are shown in Figure 4A,B. From these data, it can be inferred that a relatively small amount of FLG in the composite (3 wt %) confers the material with a low surface resistivity and a relatively high electrical conductivity (1500 S m^{-1}) that reaches values up to 7000 S m^{-1} for a 6 wt % of the FLG deposit. This electrical conductivity trend is attributed to the good percolation of the FLG sheets within the cotton matrix, a behavior similar to that previously observed in the case of CNT-based composites.^{59–61} The increased electrical conductivity of FLG@CC follows the number of coating cycles to which the hosting matrix undergoes, and it is directly attributed to the improvement of FLG sheet percolation. Noteworthy, the overall electrical conductivity of FLG@CC improves as a function of the temperature of the sample drying treatment. For instance, the electrical conductivity of a 6 wt % FLG-coated cotton cloth increases from 7000 to $13,000 \text{ S m}^{-1}$ by drying the sample at 200 °C instead of 100 °C. The FLG loading and drying temperature of the composite tune appreciably the ultimate material electrical conductivity. Such a remarkable improvement of electrical conductivity upon the

increase of the drying temperature can be explained (as above) by improved FLG sheet self-adhesion and the shrink around the cotton fibers as well as the desorption of moisture or adsorbed compounds on its surface. Indeed, the reduction of moisture trapped between graphene sheets reinforces the van der Waals contributions, hence improving the graphene interlayer connection. Anyway, high-temperature ($\geq 300 \text{ °C}$) treatments should be somehow avoided as they can alter the mechanical resistance of the composite, except for specific applications as a flame-retardant composite (see below). Hence, a compromise between drying temperature, electrical conductivity, and physical properties of the final material is mandatory to be fixed. The possibility of tuning the electrical conductivity of the FLG@CC composites by varying their (thermal) drying treatment represents an interesting tool for modulating the material chemico-physical properties and hence their ultimate technological applications. It should be stressed that such a kind of control is not available for classical metal conductors or conducting polymeric films so far.

The electrical resistance of graphene coatings translates into rapid material heating upon the application of an external potential. Accordingly, the temperature of FLG@CC was monitored using a planar thermocouple applied directly at the surface of the composite (Figure 4C). The results shown in Figure 4D show the high-temperature response of FLG@CC in terms of heating upon the application of an external potential and cooling at the open circuit. In a model experiment, 15 V dc power supply triggers rapid heating of the composite up to 95 °C within 100 s, followed by an even more rapid cooling process when the power supply is switched off. The temperature at the maximum remains relatively stable, which could be due to the 2D structure of the heater with a high heat response. The specific power (W/m^2) calculated as a function of the applied voltage is shown in Figure 4E. Devices featured by such a rapid surface heating/cooling response can find applications in several technological fields such as heated seats or lightweight/high-performance heated surfaces. At odds with traditional bulk heating, surface heating allows to get a homogeneous temperature all over the material surface with a reduced energy impact. Moreover, the generally large surface area and low thickness of the heating phase allow one to reach rapidly the steady-state temperature. These features prompted

us to explore our FLG@CC composites as highly on/off-responsive surface heaters. The large surface area and low thickness of the heating devices also provide a rapid steady-state temperature.

3.3. Synthesis of FLG@CC e-Textiles as High On/Off-Responsive Surface Heaters. For model e-textiles to be applied as surface heater devices, cotton cloths (225 cm², 15 cm × 15 cm) were coated with 2 and 4.5 wt % FLG aqueous solution by paint brushing or dip coating before being dried at 130 °C for 1 h. Afterward, all e-textiles were decorated with two copper electrodes located on opposite sides and a thin layer of Teflon was applied to their external surfaces (on the regions between the two copper electrodes). Teflon coating was used to confer a higher mechanical resistance to the composites. It allowed one to prevent the electrical conductivity loss caused by any accidental heater surface wetting and also for the security of the device. Finally, all e-textiles were heated by means of an external dc power supply.

According to the results, all heated e-textiles reach a steady-state temperature within a few tens of seconds. The target temperature value is a function of the external applied potential (*V*), and it is constantly maintained till the power supply varies or it is switched off. As shown in Figure 5A–C, for FLG@CC prepared by paint brushing (one single face is FLG-coated with an FLG loading of 2 wt %), the maximum temperature reached by the composite is 94 °C at an applied potential of 40 V dc.

On the other hand, the e-textile prepared by dip coating (both cotton faces are FLG-coated with an overall FLG loading of 4.5 wt %) (Figure 5D–F) reaches a stable surface temperature of about 50 °C already at an applied voltage of 15 V and quickly rises up to 130 °C for an applied potential of 40 V. In addition, a higher FLG loading reduces significantly the time needed to heat the composite to its maximum temperature. While the paint-brushed FLG@CC requires about 30 s to reach 94 °C (an applied potential of 40 V), the double-face-coated FLG@CC reaches 132 °C in less than 20 s. The higher the FLG loading, the higher the surface temperature reached by the composite (for a given applied potential) and the shortest the time needed to get it. Accordingly, the whole matrix-coated e-textile by dip coating can reach higher temperatures in a faster way than its single-face-coated counterpart when the same external potential is applied. Whatever is the method used for the preparation of the e-textile (paint brushing vs dip coating), the surface temperature is remarkably stable and it remains unchanged even after several on/off switching runs, hence indicating that no surface heater deterioration takes place appreciably upon use.

Overall, it is apparent that e-textiles prepared by the dip-coating method provide more homogeneously coated cotton fibers, thus ensuring improved heating efficiency to the composites.

Figure S8 shows an FLG@CC composite with 8 wt % loading by the dip-coating process which displayed a surface temperature of 83 °C under an applied voltage of 22 V. The technique also allows us to produce FLG@CC with variable dimensions depending on the downstream applications. An example of an FLG@CC composite with a dimension of 0.56 m × 0.36 m × 0.0005 m is shown in Figure S9.

3.4. FLG@CC e-Textiles as Metal-Free Thermal Markers. Invisible and flexible markers can find use in several applications both in civil and in military areas. We have shown

how the FLG@CC fabric can be used as a thermal marker with a high responsive time at a low energy input. One main advantage of the FLG@CC fabric as a thermal marker is the absence of any metal component. This feature makes our marker highly attractive, sustainable, and safe while preventing any interaction with other detection systems.

Figure 6 illustrates the application of an FLG@CC e-textile as a thermal marker. In this experiment, a series of parallel

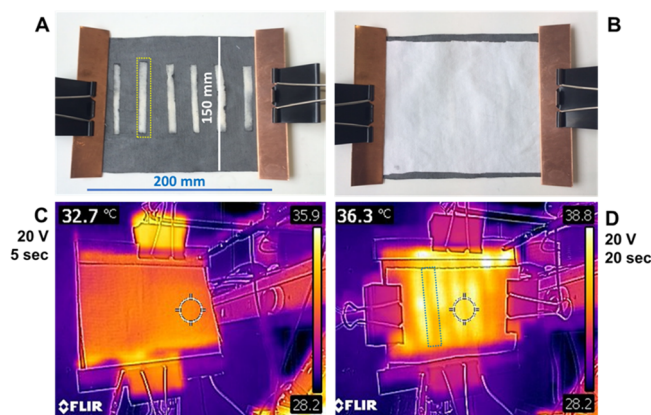


Figure 6. (A) Digital photo of the FLG/resin/CC fabric with a series of uncoated parallel strips, (B) digital photo of the assembly consisting of an FLG/resin/CC fabric and an uncoated CC fabric on the top, playing the role of a mask, and (C,D) corresponding thermal images of the marker as a function of the heating duration under an applied voltage of 20 V. The uncoated area is marked in a box for the sake of clarity.

strips were applied on the conductive fabric (Figure 6A) and a second plain textile with no FLG deposits was used to mask the e-textile surface (Figure 6B). The application of a potential (20 V) to the e-textile led to rapid heating of the hidden surface. The process was followed using a FLIR thermal camera that revealed the underneath fingerprint of the strip-decorated e-textile (Figure 6C,D). Such a technology can also allow the targeted heating of specific areas of the e-textile by playing with patterning of its electrically conductive deposits or by applying different potentials to separate conductive inlets. This will allow the display of messages or images which can be thermally mapped using an IR detector.

It can be inferred that the moderate production costs of FLG@CC fabrics along with the light weight, flexibility, and their rapid thermal response to the applied potentials can make this class of composites highly attractive as thermal markers in several technological areas such as on-site or individual thermal markers in applications nowadays. On a different perspective, an FLG-coated matrix can also be employed to preserve the heat of a body or hot object, hence reducing heat (energy) dispersion to the surrounding environment. To this aim, our FLG paint-brushing technology was successfully applied to a lab nitrile rubber glove (FLG@glove) to simplify the experiment. FLG@glove was straightforwardly prepared by coating the lab glove with a 5 g/L FLG aqueous suspension, followed by thermal stabilization of FLG deposits in an oven at 80 °C for 15 min. The FLG loading measured by weighing the glove before and after FLG coating was amounted to 0.8 wt %. Digital photos of the FLG-coated and uncoated gloves are shown in Figure 7A. The corresponding FLIR thermal images of a coated and uncoated glove are shown in Figure 7B, where



Figure 7. (A) Digital and (B) FLIR images of the uncoated and FLG-coated gloves, followed by a thermal treatment at 80 °C for 15 min. The experiments were carried out at an ambient temperature of 26 °C. The heat radiation can be clearly visualized on the FLG-coated glove which displays an orange thermal color (left) instead of a bright-yellow color for the uncoated one (right). (C) FLIR image of FLG@glove and (D) uncoated glove with almost 4 °C difference in terms of heat radiation.

657 it is evident how the FLG coating reduces the body heat loss
658 through IR radiation.

659 Indeed, FLG@glove displays a lower surface temperature
660 (30.6 °C) (Figure 7C) with a color closest to orange compared
661 to the temperature measured on the plain one (34.3 °C)
662 (Figure 7D) featuring with a color closest to bright yellow.
663 Similar to other literature precedents,^{62–64} the FLG surface
664 coating of wearable garments reduces the body heat dissipation
665 (via IR radiation) to the external environment and allows the
666 body to be maintained under thermal comfort conditions. In
667 addition, such equipment can be used to reduce the IR
668 detectable level of radiating hot bodies or objects.

669 **3.5. FLG@CC e-Circuits Prepared by Laser Ablation/
670 Graphitization.** Our methodology for the preparation of thin
671 and homogeneous FLG coating of cotton cloths has also been
672 employed in combination with a surface ablation technique for
673 the preparation of e-circuits through laser patterning^{65,66} of the
674 graphene deposit. Such a technique allows one to generate
675 electrically conductive tracks with high lateral precision for the
676 cheap production of highly flexible and versatile circuit boards
677 or smart e-textiles. The laser patterning/etching allows one to
678 groove, with an extremely high processing rate (see the
679 Materials and Methods section), the FLG deposit at different
680 depths, thus controlling and modulating the track electrical
681 resistance without damaging the host cotton matrix. In
682 addition, it is worthy to note that using the laser technique,
683 the patterns could be prepared with high lateral precision as
684 well as with a high production speed in order to cope with
685 industrial development and use.

686 In a model experiment, an FLG@CC was prepared by paint-
687 brushing one face of a cotton cloth (ca. 16 cm²) with an FLG
688 aqueous solution (5 g/L). The graphene deposit was repeated
689 twice, and FLG@CC was dried in an oven at 130 °C for 2 h
690 after each deposit. The FLG loading of the as-prepared
691 composite was 1.3 wt %, and its surface showed a mean
692 electrical resistance of 50 Ω (Figure 8A). A laser was used to
693 selectively remove a part of the FLG deposit, hence creating e-
694 textile areas with a high lateral resolution and variable electrical
695 resistance. Figure 8B illustrates an example where complete
696 FLG removal was accomplished locally by laser ablation
697 without damaging the cotton matrix underneath. As illustrated
698 in the figure, the laser-treated areas present a virtually infinite
699 electrical resistance. Similar to our previous report on
700 graphene-coated paper sheets,⁶⁵ the laser beam can also be
701 used to drive heat locally on the FLG deposits. This approach
702 does not aim at removing FLG layers but is used to increase
703 their graphitization degree through laser surface irradiation,
704 hence changing their ultimate electrical conductivity. By this
705 way, the areas at the FLG@CC surface featured by variable

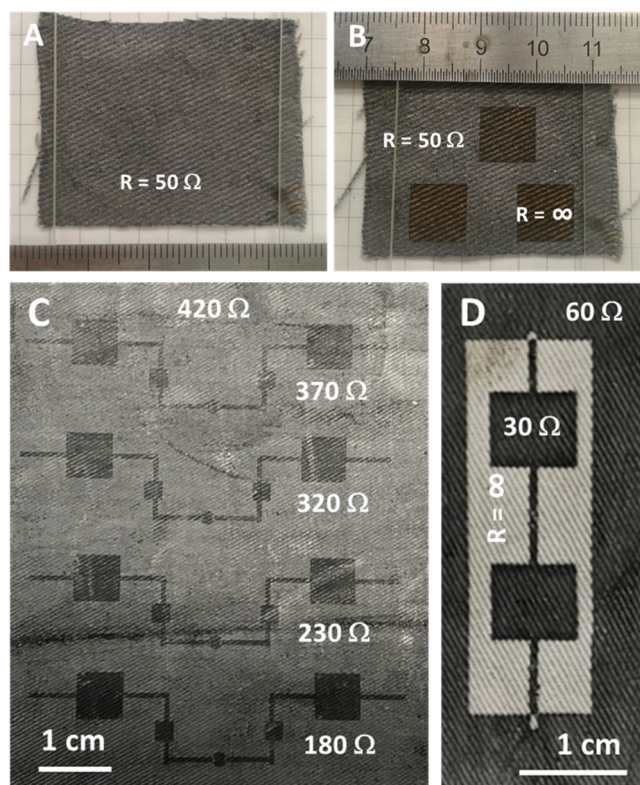


Figure 8. (A) Pristine FLG/cotton composite with an average surface resistance of $50 \pm 5 \Omega$. (B) Same FLG/cotton composite with three square areas which were etched by laser ablation showing an infinite resistance value compared to that of the untreated area. (C) Digital photo of different connectors with reducing resistance produced on FLG@CC after laser patterning and graphitization with different durations. (D) Digital photo of the same FLG@CC after patterning and local graphitization for modifying the resistance of the different areas with a high lateral resolution.

electrical resistances (from 420 down to 180 Ω) have been
created (Figure 8C). As shown in Figure 8C, the higher the
graphitization degree, the lower the local electrical resistance of
the treated e-textile area and the darker its color.

Figure 8D illustrates the combination of the two laser
treatments: laser etching (to increase the resistance of the
area) and graphitization (to decrease the resistance of the
area). By adjusting the output laser power, different electrical
connection paths featured by variable electrical resistances can
be generated, thus giving rise to real flexible electronic circuits
with a high lateral resolution. In addition, all laser treatments
can be accomplished while preserving the whole integrity of
the cotton matrix underneath.

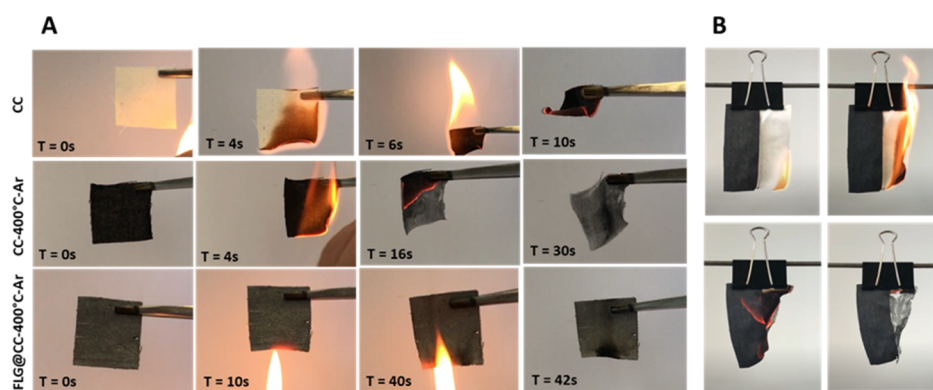


Figure 9. (A) Digital photos of the combustion behavior of the different materials in contact with a direct flame. CC: pristine cotton cloth without any treatment; CC-400°C-Ar: cotton cloth after heat treatment under argon flow at 400 °C for 1 h; FLG@CC-400°C-Ar: cotton cloth after heat treatment under argon at 400 °C for 1 h, followed by two dip-coating impregnations in an aqueous solution of FLG and oven drying at 150 °C for 30 min after each impregnation. (B) Example of the inflammable character of FLG@CC-400°C-Ar compared to that of the pristine uncoated cotton cloth stapled alongside, which steadily burns within a few seconds after contacting with a flame.

719 **3.6. FLG@CC as Flame-Retardant e-Textiles.** FLG
 720 coating of cotton cloths was finally investigated to prevent
 721 the material ignition and combustion upon its direct exposure
 722 to open flames. To this aim, FLG@CC was prepared by dip
 723 coating as follows: the cotton matrix was preliminarily treated
 724 under an inert atmosphere (Ar) at 400 °C for 1 h to remove as
 725 much as possible the oxygenated functional groups from the
 726 fiber matrix before being soaked in a 5 g/L FLG aqueous
 727 suspension and dried in an oven at 200 °C for 30 min.

728 The procedure was repeated twice to get a homogeneous
 729 coating of the cotton fibers with a final FLG loading close to 3
 730 wt %. The as-prepared dark-gray composite was exposed to an
 731 open flame, and the results are shown in Figure 9A. According
 732 to this digital sequence, the plain cotton matrix was almost
 733 entirely burned within a few seconds (10 s). The same after
 734 heat treatment under argon at 400 °C for 1 h (CC-400°C-Ar)
 735 displays a slower combustion, mostly through the smoldering
 736 mode, and becomes completely consumed after 30 s. The
 737 smoldering combustion of the sample could be explained by
 738 the absence of oxygenated functional groups which constituted
 739 the cellulose fibers after heat treatment at 400 °C. However,
 740 the remaining cotton fibers still display high affinity with
 741 oxygen and thus get consumed with time because of their low
 742 thermal stability, being totally consumed after 30 s since their
 743 contact with a direct flame. On the other hand, FLG@CC-
 744 400°C-Ar showed important flame-retardant properties,
 745 maintaining its original shape almost unaltered even after
 746 prolonged contact (40 s) with an open flame. Despite the
 747 observed glowing of the region directly in contact with the
 748 flame (due to heat absorption by FLG deposits), no material
 749 combustion took place. This flame-retardant behavior can be
 750 ascribed to the homogeneous FLG coating of cotton fibers that
 751 prevents oxygen diffusion through the textile matrix, hence
 752 conferring the composite with an extremely high oxidation
 753 resistance. These results can be attributed to the complete
 754 coverage of the cotton cloth fibers by a layer of FLG with high
 755 oxidation resistance that prevents oxygen diffusion to the inner
 756 fibers, resulting in a barrier for the flammable diffusion process.

757 In another experiment, the FLG@CC-400°C-Ar sample was
 758 stapled with an untreated/uncoated CC sample (Figure 9B).
 759 The CC sample was put in contact with a flame, and a series of
 760 snapshots were taken as a function of time to highlight the
 761 inflammable character of the graphene-coated cotton cloth.

762 FLG@CC-400°C-Ar displays significant glowing, but no
 763 combustion occurred, which confirms the high flame resistance
 764 of the composite. It is thus expected that such FLG@CC can
 765 be efficiently used as a lightweight and flexible flame barrier
 766 retardant or even a flame inhibitor for the protection of fragile
 767 structures or to protect people from flame, that is, firemen or
 768 military applications. The easy preparation method also
 769 renders FLG@CC a cost-effective material for such challenging
 770 applications.

771 Another example of the high flame resistance of the FLG@
 772 CC-400°C-Ar composite is shown in Figure S10. In such an
 773 example, FLG@CC-400°C-Ar was used as an unflammable
 774 hosting device for melting metal, that is, stain. The preformed
 775 FLG@CC composite can thus be used as a mold for making a
 776 controlled shaped metal with a low melting point.

4. CONCLUSIONS

777 Flexible composites consisting of an FLG-decorated cotton
 778 fabric with high stability and tunable electrical conductivity for
 779 use as flexible surface heaters have been synthesized. The
 780 composites displayed a high thermal response and stability
 781 against the heating and shutdown processes and confirmed
 782 their high potential for the targeted applications in the field of
 783 e-textiles. The excellent electrical and thermal properties as
 784 well as the high degree of entanglement of FLG provide a fast
 785 response, stability, and a high surface temperature even at low
 786 input power (small applied voltage). The as-synthesized
 787 composite could also be efficiently used as a metal-free
 788 thermal marker for stationary or mobile sources in both civilian
 789 and military applications. Complete flexible electronic circuits
 790 with various resistance values and connectivities can be made
 791 on one-side-coated FLG@cotton cloth using laser patterning
 792 and local graphitization without damaging the cotton cloth
 793 host substrate underneath. The low-cost production and the
 794 high performance observed render the FLG@CC fabric
 795 composite competitive compared to those using silver or
 796 metal nanoparticles available in the market. The obtained
 797 results demonstrate that thin-layer-coated FLG on a cotton
 798 cloth could be a promising candidate for low-cost wearable,
 799 flexible, and stretchable heaters under low applied voltages.
 800 These composites can be further used in other applications
 801 such as lightweight/high-performance metal-free IR reflectors
 802 to reduce the heat loss through IR radiation to the ambient

803 environment. Finally, the coating of a thermally treated cotton
804 cloth with a graphene layer also effectively prevents the
805 burning of the composite even after prolonged contact with a
806 flame, which renders such a composite highly interesting for
807 being used as a flame barrier to protect sensitive structures or
808 people from flame propagation. Work is ongoing to investigate
809 the use of such composites as dual-surface materials, that is,
810 hydrophilic cotton fibers coated with a graphene layer as heat
811 absorbers, for the water desalination process, or as graphene-
812 coated polymer fibers, with a highly rough surface and long-
813 term stability, to be used as electrical filters with a high heat
814 on/off triggering system for trapping and for inactivating living
815 matter such as viruses or bacteria.

816 ■ ASSOCIATED CONTENT

817 ■ Supporting Information

818 The Supporting Information is available free of charge at
819 <https://pubs.acs.org/doi/10.1021/acsanm.0c01861>.

820 Digital photos and contact angle of the water droplet on
821 the surface of the FLG@CC composites after coating,
822 followed by different thermal treatments; digital and
823 SEM images of the FLG@CC composites after the
824 repeated folding process; XPS survey spectra of pristine
825 FLG, the CC, and the FLG@CC composite; XPS C 1s
826 spectra of FLG, the CC, and FLG@CC; high-resolution
827 XPS O 1s spectra of FLG, the CC, and FLG@CC;
828 digital photos of the FLG@CC composite immersed
829 inside a mixture of ethanol/water (20:80 v/v %) and the
830 same after sonication for 30 min; thermal behavior of
831 FLG@CC (8 wt % loading) under different applied
832 voltages; digital photo of the FLG@CC composites with
833 large dimensions produced through the dip-coating
834 process with an FLG aqueous solution of 10 g L⁻¹;
835 experiments evidencing the high oxidative resistance of
836 the FLG@CC composites; and area and position of C 1s
837 peak components of the three samples (PDF)

838 ■ AUTHOR INFORMATION

839 Corresponding Authors

840 **Housseinou Ba** – Institute of Chemistry and Processes for
841 Energy, Environment and Health (ICPEES), UMR 7515
842 CNRS—University of Strasbourg, Strasbourg Cedex 02 67087,
843 France; orcid.org/0000-0001-6263-0671; Email: hba@blackleaf.fr

845 **Giuliano Giambastiani** – Institute of Chemistry and Processes
846 for Energy, Environment and Health (ICPEES), UMR 7515
847 CNRS—University of Strasbourg, Strasbourg Cedex 02 67087,
848 France; Institute of Chemistry of OrganoMetallic Compounds,
849 ICCOM-CNR and Consorzio INSTM, Florence 50019, Italy;
850 Kazan Federal University, Kazan 420008, Russian Federation;
851 orcid.org/0000-0002-0315-3286;
852 Email: giuliano.giambastiani@iccom.cnr.it

853 **Cuong Pham-Huu** – Institute of Chemistry and Processes for
854 Energy, Environment and Health (ICPEES), UMR 7515
855 CNRS—University of Strasbourg, Strasbourg Cedex 02 67087,
856 France; Email: cuong.pham-huu@unistra.fr

857 Authors

858 **Lai Truong-Phuoc** – Institute of Chemistry and Processes for
859 Energy, Environment and Health (ICPEES), UMR 7515
860 CNRS—University of Strasbourg, Strasbourg Cedex 02 67087,
861 France

Vasiliki Papaefthimiou – Institute of Chemistry and Processes 862
for Energy, Environment and Health (ICPEES), UMR 7515 863
CNRS—University of Strasbourg, Strasbourg Cedex 02 67087, 864
France 865

Christophe Sutter – Institute of Chemistry and Processes for 866
Energy, Environment and Health (ICPEES), UMR 7515 867
CNRS—University of Strasbourg, Strasbourg Cedex 02 67087, 868
France 869

Sergey Pronkin – Institute of Chemistry and Processes for 870
Energy, Environment and Health (ICPEES), UMR 7515 871
CNRS—University of Strasbourg, Strasbourg Cedex 02 67087, 872
France 873

Armel Bahouka – MANIPULSE, Ilkirch 67400, France 874

Yannick Lafue – Institute of Chemistry and Processes for Energy, 875
Environment and Health (ICPEES), UMR 7515 CNRS— 876
University of Strasbourg, Strasbourg Cedex 02 67087, France 877

Lam Nguyen-Dinh – University of Science and Technology, The 878
University of Da Nang, Da Nang 550000, Vietnam 879

Complete contact information is available at: 880
<https://pubs.acs.org/10.1021/acsanm.0c01861> 881

882 Author Contributions

883 H.B.: conceptualization, investigation, writing—original draft 883
and editing, and visualization. L.T.-P.: investigation. V.P.: 884
investigation and editing. C.S.: conceptualization and inves- 885
tigation. S.P.: investigation. A.B.: investigation and writing— 886
original draft. Y.L.: investigation. L.N.-D.: conceptualization. 887
G.G.: conceptualization and writing—original draft. C.P.-H.: 888
conceptualization, supervision, writing—original draft and 889
editing, and project administration. 890

891 Notes

892 The authors declare no competing financial interest. 892

893 ■ ACKNOWLEDGMENTS

894 We acknowledge the financial support from the SATT 894
Conectus through the GRAPHICS project. G.G. and C.P.-H. 895
thank the TRAINER project (Catalysts for Transition to 896
Renewable Energy Future) of the “Make our Planet Great 897
Again” program (ref. ANR-17-MPGA-0017) for support. The 898
SEM and TEM experiments are carried out at the facilities of 899
the ICPEES (UMR 7515) and the IPCMS (UMR 7504). Prof. 900
G. Schlatter and T. Romero (ICPEES) are gratefully 901
acknowledged for SEM experiments. Dr. W. Baaziz and Prof. 902
O. Ersen (IPCMS, UMR 7504) are gratefully acknowledged 903
for performing TEM experiments. 904

905 ■ REFERENCES

- 896 (1) Custodio, V.; Herrera, F.; López, G.; Moreno, J. A Review on 906
Architectures and Communications Technologies for Wearable 907
Health-Monitoring Systems. *Sensors* **2012**, *12*, 13907–13946. 908
- 899 (2) Coosemans, J.; Hermans, B.; Puers, R. Integrating wireless ECG 909
monitoring in textiles. *Sens. Actuators, A* **2006**, *130–131*, 48–53. 910
- 911 (3) Löfhede, J.; Seoane, F.; Thordstein, M. Textile Electrodes for 911
EEG Recording - A Pilot Study. *Sensors* **2012**, *12*, 16907–16919. 912
- 913 (4) Sibinski, M.; Jakubowska, M.; Sloma, M. Flexible Temperature 913
Sensors on Fibers. *Sensors* **2010**, *10*, 7934–7946. 914
- 915 (5) Bai, S.; Zhang, L.; Xu, Q.; Zheng, Y.; Qin, Y.; Wang, Z. L. Two 915
dimensional woven nanogenerator. *Nano Energy* **2013**, *2*, 749–753. 916
- 917 (6) Lee, Y.-H.; Kim, J.-S.; Noh, J.; Lee, I.; Kim, H. J.; Choi, S.; Seo, 917
J.; Jeon, S.; Kim, T.-S.; Lee, J.-Y. Wearable Textile Battery 918
Rechargeable by Solar Energy. *Nano Lett.* **2013**, *13*, 5753–5761. 919
- 920 (7) Chiechi, R. C.; Havenith, R. W. A.; Hummelen, J. C.; Koster, L. 920
J. A.; Loi, M. A. Modern plastic solar cells: materials, mechanisms and 921
modeling. *Mater. Today* **2013**, *16*, 281–289. 922

- 923 (8) Liu, W.-w.; Yan, X.-B.; Lang, J.-W.; Peng, C.; Xue, Q.-J. Flexible
924 and conductive nanocomposite electrode based on graphene sheets
925 and cotton cloth for supercapacitor. *J. Mater. Chem. A* **2012**, *22*,
926 17245–17253.
- 927 (9) Pahalagedara, L. R.; Siriwardane, I. W.; Tissera, N. D.; Wijesena,
928 R. W.; Nalin de Silva, K. M. Carbon black functionalized stretchable
929 conductive fabrics for wearable heating applications. *RSC Adv.* **2017**,
930 *7*, 19174–19180.
- 931 (10) Stoppa, M.; Chiolerio, A. Wearable Electronics and Smart
932 Textiles: A Critical Review. *Sensors* **2014**, *14*, 11957–11992.
- 933 (11) Park, S.; Jayaraman, S. Smart Textiles: Wearable Electronic
934 Systems. *MRS Bull.* **2003**, *28*, 585–591.
- 935 (12) Gniotek, K.; Krucinska, I. The basic problems of textronics.
936 *Fibres Text. East. Eur.* **2004**, *12*, 13–16.
- 937 (13) Kirstein, T.; Tröster, G.; Lukowicz, P. Wearable Systems for
938 Health Care Applications. *Methods Inf. Med.* **2004**, *43*, 232–238.
- 939 (14) Avila, A. G.; Hinestroza, J. P. Smart textiles: tough cotton. *Nat.*
940 *Nanotechnol.* **2008**, *3*, 458–459.
- 941 (15) De Rossi, D. A logical step. *Nat. Mater.* **2007**, *6*, 328–329.
- 942 (16) Service, R. F. Electronic Textiles Charge Ahead. *Science* **2003**,
943 *301*, 909–911.
- 944 (17) Hu, L.; Pasta, M.; La Mantia, F.; Cui, L.; Jeong, S.; Deshazer,
945 H. D.; Choi, J. W.; Han, S. M.; Cui, Y. Stretchable, Porous, and
946 Conductive Energy Textiles. *Nano Lett.* **2010**, *10*, 708–714.
- 947 (18) Ismar, E.; Bahadir, S. K.; Kalaoglu, F.; Koncar, V. Futuristic
948 Clothes: Electronic textiles and Wearable Technologies. *Glob. Chall.*
949 **2020**, *4*, 1900092.
- 950 (19) Karim, N.; Afroj, S.; Tan, S.; He, P.; Fernando, A.; Carr, C.;
951 Novoselov, K. S. Scalable Production of Graphene-Based Wearable E-
952 Textiles. *ACS Nano* **2017**, *11*, 12266–12275.
- 953 (20) Paredes, J. I.; Villar-Rodil, S. Biomolecule-assisted exfoliation
954 and dispersion of graphene and other two-dimensional materials: a
955 review of recent progress and applications. *Nanoscale* **2016**, *8*, 15389–
956 15413.
- 957 (21) Chabot, V.; Kim, B.; Sloper, B.; Tzoganakis, C.; Yu, A. High
958 yield production and purification of few-layer graphene by Gum
959 Arabic assisted physical sonication. *Sci. Rep.* **2013**, *3*, 1378.
- 960 (22) Geim, A. K.; Novoselov, K. S. The rise of graphene. *Nat. Mater.*
961 **2007**, *6*, 183–191.
- 962 (23) Park, S.; Ruoff, R. S. Chemical methods for the production of
963 graphenes. *Nat. Nanotechnol.* **2009**, *4*, 217–224.
- 964 (24) Allen, M. J.; Tung, V. C.; Kaner, R. B. Honeycomb carbon: a
965 review of graphene. *Chem. Rev.* **2010**, *110*, 132–145.
- 966 (25) Shao, Y.; Wang, J.; Wu, H.; Liu, J.; Aksay, I. A.; Lin, Y.
967 Graphene based electrochemical sensors and biosensors: a review.
968 *Electroanalysis* **2010**, *22*, 1027–1036.
- 969 (26) Coroş, M.; Poyccean, F.; Magerusan, L.; Socaci, C.; Pruneanu,
970 S. A brief overview on synthesis and applications of graphene and
971 graphene-based nanomaterials. *Front. Mater. Sci.* **2019**, *13*, 23–32.
- 972 (27) Janowska, I.; Chizari, K.; Ersen, O.; Zafeiratou, S.; Soubane, D.;
973 Da Costa, V.; Speisser, V.; Boeglin, C.; Houllé, M.; Bégin, D.; Plee,
974 D.; Ledoux, M.-J.; Pham-Huu, C. Microwaves synthesis of large few-
975 layer graphene sheets in aqueous solution of ammonia. *Nano Res.*
976 **2010**, *3*, 126–137.
- 977 (28) Ba, H.; Truong-Phuoc, L.; Pham-Huu, C.; Luo, W.; Baaziz, W.;
978 Romero, T.; Janowska, I. Colloid Approach to the Sustainable Top-
979 Down Synthesis of Layered Materials. *ACS Omega* **2017**, *2*, 8610–
980 8617.
- 981 (29) Bae, S.; Kim, H.; Lee, Y.; Xu, X.; Park, J.-S.; Zheng, Y.;
982 Balakrishnan, J.; Lei, T.; Ri Kim, H.; Song, Y. I.; Kim, Y.-J.; Kim, K. S.;
983 Özyilmaz, B.; Ahn, J.-H.; Hong, B. H.; Iijima, S. Roll-to-roll
984 production of 30-inch graphene films for transparent electrodes.
985 *Nat. Nanotechnol.* **2010**, *5*, 574–578.
- 986 (30) Pang, S.; Fernandez, Y.; Feng, X.; Müllen, K. Graphene as
987 Transparent Electrode Material for Organic Electronics. *Adv. Mater.*
988 **2011**, *23*, 2779–2795.
- 989 (31) Bae, J. J.; Lim, S. C.; Han, G. H.; Jo, Y. W.; Doung, D. L.; Kim,
990 E. S.; Chae, S. J.; Huy, T. Q.; Van Luan, N.; Lee, Y. H. Heat
Dissipation of Transparent Graphene Defoggers. *Adv. Funct. Mater.* **991**
2012, *22*, 4819–4826. 992
- (32) Kang, J.; Kim, H.; Kim, K. S.; Lee, S.-K.; Bae, S.; Ahn, J.-H.;
993 Kim, Y.-J.; Choi, J.-B.; Hong, B. H. High-Performance Graphene-
994 Based Transparent Flexible Heaters. *Nano Lett.* **2011**, *11*, 5154–5158. 995
- (33) Yang, X.; Zhu, J.; Qiu, L.; Li, D. Bioinspired Effective
996 Prevention of Restacking in Multilayered Graphene Films: Towards
997 the Next Generation of High-Performance Supercapacitors. *Adv.*
998 *Mater.* **2011**, *23*, 2833–2838. 999
- (34) Ba, H.; Truong-Phuoc, L.; Liu, Y.; Duong-Viet, C.; Nhut, J.-M.;
1000 Nguyen-Dinh, L.; Granger, P.; Pham-Huu, C. Hierarchical carbon
1001 nanofibers/graphene composite containing nanodiamonds as metal-
1002 free catalyst for direct dehydrogenation of ethylbenzene. *Carbon*
1003 **2016**, *96*, 1060–1069. 1004
- (35) Wang, B.; Cunnning, B. V.; Kim, N. Y.; Kargar, F.; Park, S. Y.; Li,
1005 Z.; Joshi, S. R.; Peng, L.; Modepalli, V.; Chen, X.; Shen, Y.; Seong, W.
1006 K.; Kwon, Y.; Jang, J.; Shi, H.; Gao, C.; Kim, G. H.; Shin, T. J.; Kim,
1007 K.; Kim, J. Y.; Balandin, A. A.; Lee, Z.; Ruoff, R. S. Ultrastiff, Strong,
1008 and Highly Thermally Conductive Crystalline Graphitic Films with
1009 Mixed Stacking Order. *Adv. Mater.* **2019**, *31*, 1903039. 1010
- (36) Ilanchezhian, P.; Zakirov, A. S.; Kumar, G. M.; Yuldashev, S.
1011 U.; Cho, H. D.; Kang, T. W.; Mamadalimov, A. T. Highly efficient
1012 CNT functionalized cotton fabrics for flexible/wearable heating
1013 applications. *RSC Adv.* **2015**, *5*, 10697–10702. 1014
- (37) Hyde, G. K.; Park, K. J.; Stewart, S. M.; Hinestroza, J. P.;
1015 Parsons, G. N. Atomic Layer Deposition of Conformal Inorganic
1016 Nanoscale Coatings on Three-Dimensional Natural Fiber Systems:
1017 Effect of Surface Topology on Film Growth Characteristics. *Langmuir*
1018 **2007**, *23*, 9844–9849. 1019
- (38) Shim, B. S.; Chen, W.; Doty, C.; Xu, C.; Kotov, N. A. Smart
1020 Electronic Yarns and Wearable Fabrics for Human Biomonitoring
1021 made by Carbon Nanotube Coating with Polyelectrolytes. *Nano Lett.*
1022 **2008**, *8*, 4151–4157. 1023
- (39) Nowack, B.; David, R. M.; Fissan, H.; Morris, H.; Shatkin, J. A.;
1024 Stintz, M.; Zepp, R.; Brouwer, D. Potential release scenarios for
1025 carbon nanotubes used in composites. *Environ. Int.* **2013**, *59*, 1–11. 1026
- (40) Gonçalves, A. G.; Jarrais, B.; Pereira, C.; Morgado, J.; Freire, C.;
1027 Pereira, M. F. R. Functionalization of textiles with multi-walled carbon
1028 nanotubes by a novel dyeing-like process. *J. Mater. Sci.* **2012**, *47*,
1029 5263–5275. 1030
- (41) Nowack, B.; Ranville, J. F.; Diamond, S.; Gallego-Urrea, J. A.;
1031 Metcalfe, C.; Rose, J.; Horne, N.; Koelmans, A. A.; Klaine, S. J.
1032 Potential scenarios for nanomaterial release and subsequent alteration
1033 in the environment. *Environ. Toxicol. Chem.* **2012**, *31*, 50–59. 1034
- (42) Xu, Y.; Cao, H.; Xue, Y.; Li, B.; Cai, W. Liquid-Phase
1035 Exfoliation of Graphene: An Overview on Exfoliation Media,
1036 Techniques, and Challenges. *Nanomaterials* **2018**, *8*, 942. 1037
- (43) Liu, Z.; Zhang, H.; Eredia, M.; Qiu, H.; Baaziz, W.; Ersen, O.;
1038 Ciesielski, A.; Bonn, M.; Wang, H. I.; Samorì, P. Water-Dispersed
1039 High-Quality Graphene: A Green Solution for Efficient Energy
1040 Storage Applications. *ACS Nano* **2019**, *13*, 9431–9441. 1041
- (44) Ma, H.; Shen, Z. Exfoliation of graphene nanosheets in aqueous
1042 media. *Ceram. Int.* **2020**, *46*, 21873–21887. 1043
- (45) BeMiller, J. N. *Carbohydrate Chemistry for Food Scientists*, 3rd
1044 ed.; BeMiller, J. N., Ed.; AACC International Press, 2019; pp 313–
1045 321. 1046
- (46) Hirst, E. L.; Dunstan, S. 476. The structure of karaya gum
1047 (*Cochlospermum gossypium*). *J. Chem. Soc.* **1953**, 2332–2337. 1048
- (47) Suslick, K. S. Sonochemistry. *Science* **1990**, *247*, 1439–1445. 1049
- (48) Hsieh, Y.-L. Chemical structure and properties of cotton. In
1050 *Cotton: Science and Technology*; Gordon, S., Hsieh, Y.-L., Eds.;
1051 Woodhead Publishing Limited: Cambridge, 2007; pp 3–34. 1052
- (49) Lujan-Medina, G. A.; Ventura, J.; Ceniceros, A. C. L.; Valdés, J.
1053 A. A.; Boone-Villa, D.; Aguilar, C. N. Karaya gum: General topics and
1054 applications. *Macromol.: Indian J.* **2013**, *9*, 111–116. 1055
- (50) Mukherjee, T.; Lerma-Reyes, R.; Thompson, K. A.; Schrick, K.
1056 Making Glue From Seeds and Gums: Working With Plant-Based
1057 Polymers to Introduce Students to Plant Biochemistry. *Biochem. Mol.*
1058 *Biol. Educ.* **2019**, *47*, 468–475. 1059

- 1060 (51) Bøggild, P. The war on fake graphene. *Nature* **2018**, *562*, 502–
1061 503.
- 1062 (52) Kauling, A. P.; Seefeldt, A. T.; Pisoni, D. P.; Pradeep, R. C.;
1063 Bentini, R.; Oliveira, R. V. B.; Novoselov, K. S.; Castro Neto, A. H.
1064 The Worldwide Graphene Flake Production. *Adv. Mater.* **2018**, *30*,
1065 1803784.
- 1066 (53) Hertel, T.; Walkup, R. E.; Avouris, P. Deformation of carbon
1067 nanotubes by surface van der Waals forces. *Phys. Rev. B: Condens.*
1068 *Matter Mater. Phys.* **1998**, *58*, 13870–13873.
- 1069 (54) Wang, S.; Zhang, Y.; Abidi, N.; Cabrales, L. Wettability and
1070 Surface Free Energy of Graphene Films. *Langmuir* **2009**, *25*, 11078–
1071 11081.
- 1072 (55) Karim, N.; Zhang, M.; Afroj, S.; Koncherry, V.; Potluri, P.;
1073 Novoselov, K. S. Graphene-based surface heater for de-icing
1074 applications. *RSC Adv.* **2018**, *8*, 16815–16823.
- 1075 (56) Palmieri, V.; Papi, M. Can graphene take part in the fight
1076 against COVID-19? *Nano Today* **2020**, *33*, 100883.
- 1077 (57) Xia, W.; Wang, Y.; Bergsträßer, R.; Kundu, S.; Muhler, M.
1078 Surface characterization of oxygen-functionalized multi-walled carbon
1079 nanotubes by high-resolution X-ray photoelectron spectroscopy and
1080 temperature-programmed desorption. *Appl. Surf. Sci.* **2007**, *254*, 247–
1081 250.
- 1082 (58) Baaziz, W.; Truong-Phuoc, L.; Duong-Viet, C.; Melinte, G.;
1083 Janowska, I.; Papaefthimiou, V.; Ersen, O.; Zafeiratos, S.; Begin, D.;
1084 Begin-Colin, S.; Pham-Huu, C. Few layer graphene decorated with
1085 homogeneous magnetic Fe₃O₄ nanoparticles with tunable covering
1086 densities. *J. Mater. Chem. A* **2014**, *2*, 2690–2700.
- 1087 (59) Zhang, W.; Tan, Y. Y.; Wu, C.; Ravi, S.; Silva, P. Self-assembly
1088 of single walled carbon nanotubes onto cotton to make conductive
1089 yarn. *Particuology* **2012**, *10*, 517–521.
- 1090 (60) Ba, H.; Sutter, C.; Bahouka, A.; Lafue, Y.; Nguyen-Dinh, L.;
1091 Pham-Huu, C. Method for Manufacturing a Conductive Composite
1092 Comprising at Least One Surface Layer Comprising Multi-Sheet
1093 Graphene. WO 2020079372 A1, 2020.
- 1094 (61) Ba, H.; Bahouka, A.; Lafue, Y.; Pham-Huu, C. Method for
1095 Producing, Applying and Fixing a Multilayer Surface Coating on a
1096 Host Substrate, and Host Substrate assembly which can be Obtained
1097 by Said Method. WO 2020109380 A1, 2020.
- 1098 (62) Hsu, P.-C.; Liu, X.; Liu, C.; Xie, X.; Lee, H. R.; Welch, A. J.;
1099 Zhao, T.; Cui, Y. Personal thermal management by metallic nanowire-
1100 coated textile. *Nano Lett.* **2015**, *15*, 365–371.
- 1101 (63) Cai, L.; Song, A. Y.; Wu, P.; Hsu, P.-C.; Peng, Y.; Chen, J.; Liu,
1102 C.; Catrysse, P. B.; Liu, Y.; Yang, A.; Zhou, C.; Zhou, C.; Fan, S.; Cui,
1103 Y. Warming up human body by nanoporous metallized polyethylene
1104 textile. *Nat. Commun.* **2017**, *8*, 496.
- 1105 (64) Salihoglu, O.; Uzlu, H. B.; Yakar, O.; Aas, S.; Balci, O.;
1106 Kakenov, N.; Balci, S.; Olcum, S.; Süzer, S.; Kocabas, C. Graphene-
1107 Based Adaptive Thermal Camouflage. *Nano Lett.* **2018**, *18*, 4541–
1108 4548.
- 1109 (65) Ba, H.; Sutter, C.; Zafeiratos, S.; Bahouka, A.; Lafue, Y.;
1110 Nguyen-Dinh, L.; Romero, T.; Pham-Huu, C. Foldable flexible
1111 electronics based on few-layer graphene coated paper composites.
1112 *Carbon* **2020**, *167*, 169–180.
- 1113 (66) Mackenzie, D. M. A.; Buron, J. D.; Whelan, P. R.; Jessen, B. S.;
1114 Silajđić, A.; Pesquera, A.; Centeno, A.; Zurutuza, A.; Bøggild, P.;
1115 Petersen, D. H. Fabrication of CVD graphene-based devices via laser
1116 ablation for wafer-scale characterization. *2D Mater.* **2015**, *2*, 045003.